Journal of Applied Polymer Science

Damping Mechanism and Different Modes of Molecular Motion Through the Glass Transition of Chlorinated Butyl Rubber and Petroleum Resin Blends

Fengshun Zhang,[1] Guansong He,[1] Kangming Xu,[1] Hong Wu,[1] Shaoyun Guo,[1] Chaoliang Zhang[2]

[1]The State Key Laboratory of Polymer Materials Engineering, Polymer Research Institute of Sichuan University, Chengdu, People's Republic of China

[2]State Key Laboratory of Oral Diseases, West China Hospital of Stomatology, Sichuan University, People's Republic of China

Correspondence to: H. Wu (E-mail: wh@scu.edu.cn)

ABSTRACT: To further investigate the effect of petroleum resin on damping mechanism and different modes of motion of chlorinated butyl rubber (CIIR), two kinds of petroleum resins with different molecular structures, aliphatic C5 resin and aromatic C9 resin, were incorporated into CIIR. The experimental results showed that the aliphatic C5 resin exhibited a better miscibility with CIIR, compared with aromatic C9 resin. With increase in the content of the C5 resin, the α process and the α' process of CIIR moved to the higher temperature but to different extents, and the effective damping temperature range was broadened remarkably. The CIIR/C9 resin blends showed two loss peaks, which corresponded to the CIIR matrix and the C9 resin dispersed phase, respectively. The C9 resin neither moved different relaxation modes of CIIR to room temperature nor enhanced the value of the loss damping peak.
 J. Appl. Polym. Sci. **2014**, *131*, 40464.

KEYWORDS: morphology; rubber; glass transition; phase behavior

Received 12 November 2013; accepted 17 January 2014
DOI: 10.1002/app.40464

INTRODUCTION

Viscoelastic polymers used as damping materials have attracted considerable attention recently for converting vibration and noise energy to heat energy. The loss tangent (tan δ), defined by the ratio E″/E′ of loss (E″) and storage modulus (E′), can be used as a measure of the vibration energy dissipation.[1,2] Usually, the excellent damping materials are usually desirable to have high values of tan δ over wide temperature and frequency ranges, especially, at the transition region from glassy to rubbery state. However, the glass transitions of homopolymers are generally restricted to a relatively narrow temperature region. A great many efforts have been devoted to broaden the effective damping temperature range of polymer.[3–6] One of the most conventional ways is the binary and ternary blends of polymers having different glass transition temperatures.

The chlorinated butyl rubber (CIIR) is well known for its higher energy absorptivity and lower molecular mobility comparing with any other polymers. As firstly discovered by Ferry et al.,[7] CIIR shows a unique relaxation behavior: the tan δ curve of CIIR reveals an asymmetrical double-peak structure with a maximum on the high-temperature side and an additional shoulder on the other side. Recently, Plazek[8] and Huang[9,10] examined that different modes of molecular motion contribute to the transition region from local segmental motion (glass transition), sub-Rouse modes, and Rouse modes. However, CIIR utilized as damping material is often limited, as all the loss peaks of the three different modes of molecular motion appear at lower temperature zone than room temperature. Hence, there are considerable researches, which have been focused on extending the damping functional region of CIIR toward a high-temperature area. For example, Liao and coworkers[11] prepared a series of dynamically cured butyl rubber/polypropylene blends, whose loss peaks of the blends tend to shift toward high temperature. However, tan δ_{max} is not over 0.35, as the maximum of loss peak is suppressed by polypropylene. Some studies have also showed that the maximum can be easily suppressed by the addition of other polymers or inorganic fillers, such as polyacrylates,[12] polystyrene,[13] and montmorillonite,[14] while the shoulder is less affected.

In recent years, it was found that the petroleum resins, kinds of amorphous polymers of low molecular weight (from 300 to 3000), exhibit glassy states at room temperature and[15] have great potential in practical damping application, based on the studies of the dynamic mechanical properties of its blends with elastomers.[16,17] Wu and coworkers investigated the CIIR/petroleum

resins blends, which only show a single tan δ peak; and with increasing the content of petroleum resins, the loss peak increases and the peak location shifts to higher temperature.[5,6]

However, the damping mechanism of such CIIR/petroleum resin blend has not been clear yet, because petroleum resins have various and complex structure types. Therefore, in order to further investigate the effect of petroleum resin on the CIIR molecular motion and damping mechanism, two kinds of petroleum resins (C5 and C9) with different molecular structures are incorporated into CIIR in this article. C5 resin is an aliphatic hydrocarbon resin of five carbon atoms per monomer, and C9 resin is an aromatic hydrocarbon resin of nine carbon atoms per monomer. Due to different molecular structures of aliphatic C5 resin and aromatic hydrocarbon C9 resin, the miscibility between C5 resin and CIIR is distinct from that of C9 resin and CIIR; as a result, the phase domain structures are different. This inspires us to further explore how the different modes of molecular motion of the CIIR and damping property are affected by different phase domain structures. For this purpose, various CIIR matrix damping materials with different C5 or C9 petroleum resin contents have been prepared, and the dynamic mechanical analysis (DMA), differential scanning calorimetry (DSC), and scanning electron microscopy (SEM) are used to characterized the damping materials.

EXPERIMENTAL

Materials

The chlorinated butyl rubber (CIIR, product code: CBK 139) with a chlorination concentration of 1.2% was from Nizhnekamsk (Russia). The aliphatic C5 petroleum resin (product code: A2100) was from Puyang Ruisen Petroleum Resin Factory (China). The aromatic C9 resin (product code: PR-110) was from Shandong Qilong chemical Co., Ltd., China.

Specimens Preparation

A laboratory-scale mixer equipped with a pair of roller blades was used for blending. Blends of CIIR with different petroleum resin contents (0–100 phr) were prepared via mechanical mixing at room temperature for 8 min; the blends were compression molded to form sheets 3 mm in thickness under a pressure of 10 MPa for 10 min at 130°C.

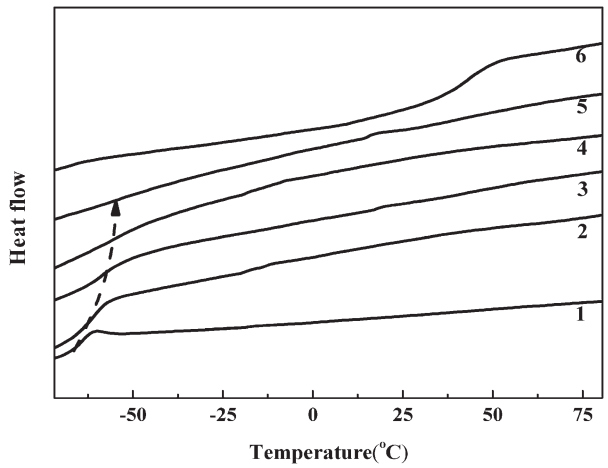

Figure 1. Heat flow curves of CIIR and CIIR/C5 resin blends with different contents, 1: CIIR, 2: CIIR/25 phr C5 resin, 3: CIIR/50 phr C5 resin, 4: CIIR/75 phr C5 resin, 5: CIIR/100 phr C5 resin, 6: C5 resin. The arrow shows the increase of Tg of CIIR with the increase of C5 resin content.

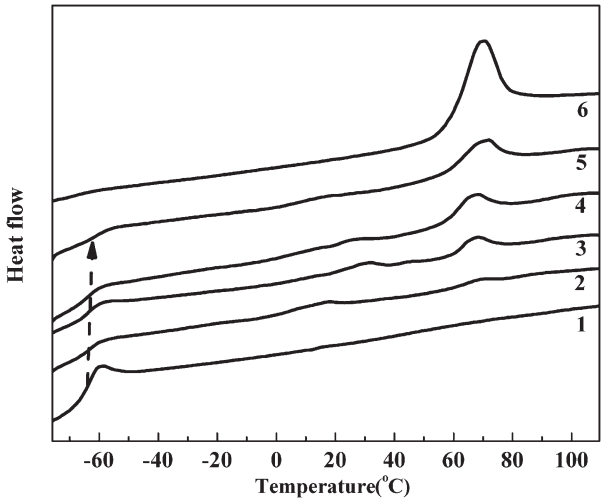

Figure 2. Heat flow curves of CIIR and CIIR/C9 resin blends with different contents, 1: CIIR, 2: CIIR/25 phr C9 resin, 3: CIIR/50 phr C9 resin, 4: CIIR/75 phr C9 resin, 5: CIIR/75 phr C9 resin, 6: C9 resin. The arrow shows the slight increase of Tg of CIIR with the increase of C9 resin content.

Dynamic Mechanical Analysis

DMA was measured by TA Q800 (TA company, USA) analyzer under a heating rate of 3°C/min within a temperature range of −80°C to 130°C and a frequency of 10 Hz for temperature scanning. The samples were trimmed to dimensions of 15 mm in length, 10 mm in width, and 2 mm in thickness.

Scanning Electron Microscopy Analysis

Preparation of sample for observation of morphology with SEM (JSM-5900LV, Japan) was carried out as follows: The samples were fractured in liquid nitrogen, then the surface was coated with gold by vacuum deposition, and the measurements utilized SEM at an accelerating voltage of 20 kV.

Differential Scanning Calorimetry

DSC test was conducted on a Q20 calorimeter (TA Instruments). The sample was cooled to −80°C from room temperature at a cooling rate of 10°C/min and stabilized for 5 min, and then heated at a heating rate of 10°C/min to 130°C. The glass transition temperature was determined as the midpoint of the glass transition region of the heat flow curve.

RESULTS AND DISCUSSION

Glass Transition of CIIR/Petroleum Resins blends

The DSC is used to evaluate the miscibility of different structure petroleum resins with the CIIR matrix and their influence on the overall dynamics of the polymer matrix. As shown in Figures 1 and 2, the glass transition temperature of aliphatic C5 resin and aromatic hydrocarbon C9 resin are 44.4°C and 65.2°C, respectively: Both are much higher than the glass transition temperature of CIIR, which is −62.6°C. For the CIIR/C5 resin blends, with increasing the content of C5 resin, the glass

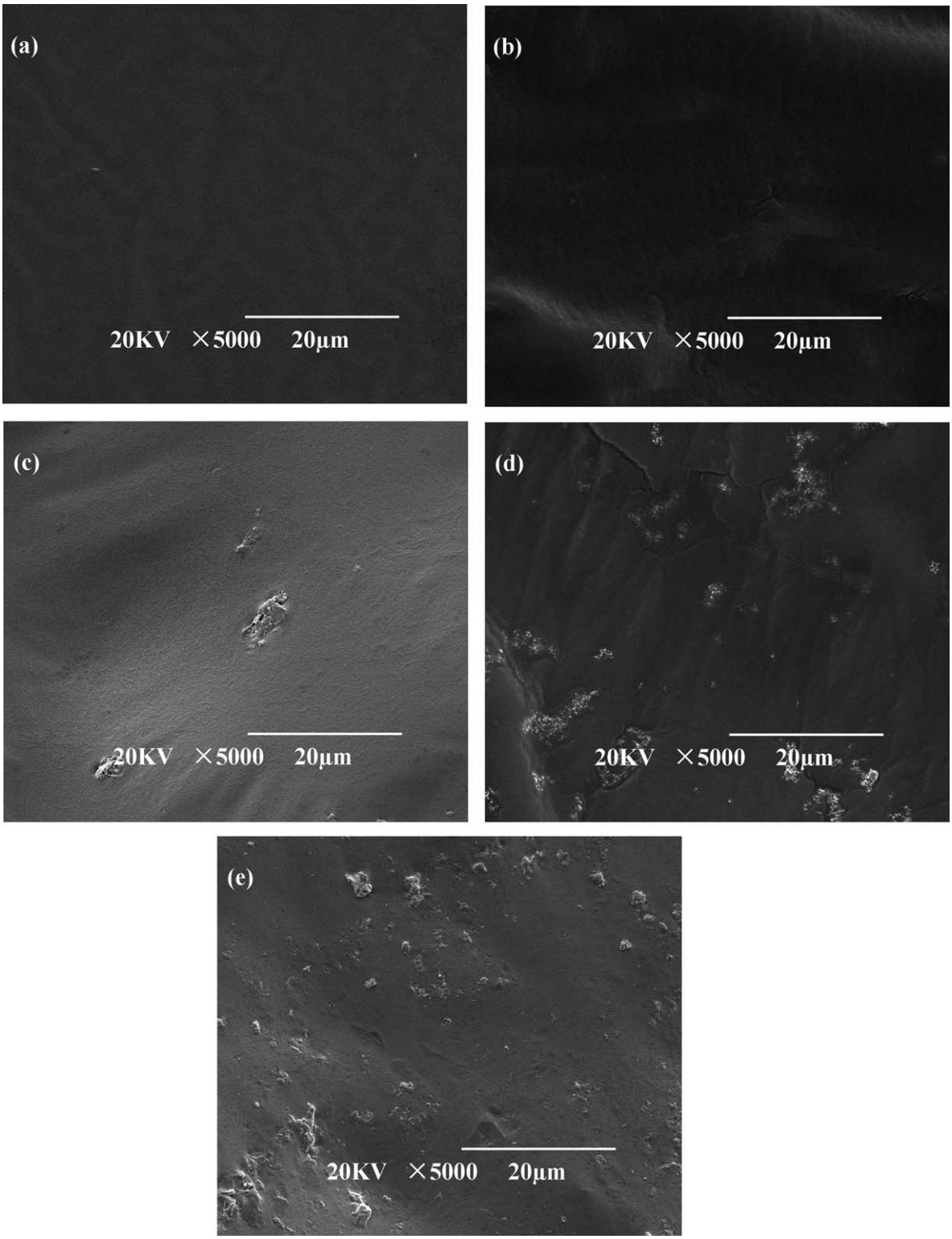

Figure 3. SEM image of CIIR with different C5 resin contents: (a) CIIR, (b) CIIR/25 phr C5 resin, (c) CIIR/50 phr C5 resin, (d) CIIR/75 phr C5 resin, (e) CIIR/100 phr C5 resin.

transition of CIIR moves to high temperature, but there is no signal that corresponds to the glass transition of C5 resin from the curves of Figure 1. According to the literature,[18] the glass transition is the cooperative rearranging of local segments and is sensitive to the change of local arrangement of molecular chains. Hence, the change of the glass transition indicates that the C5 resin exhibit a good miscibility with CIIR. Moreover, it is worth noting that the transition breadths of CIIR in the

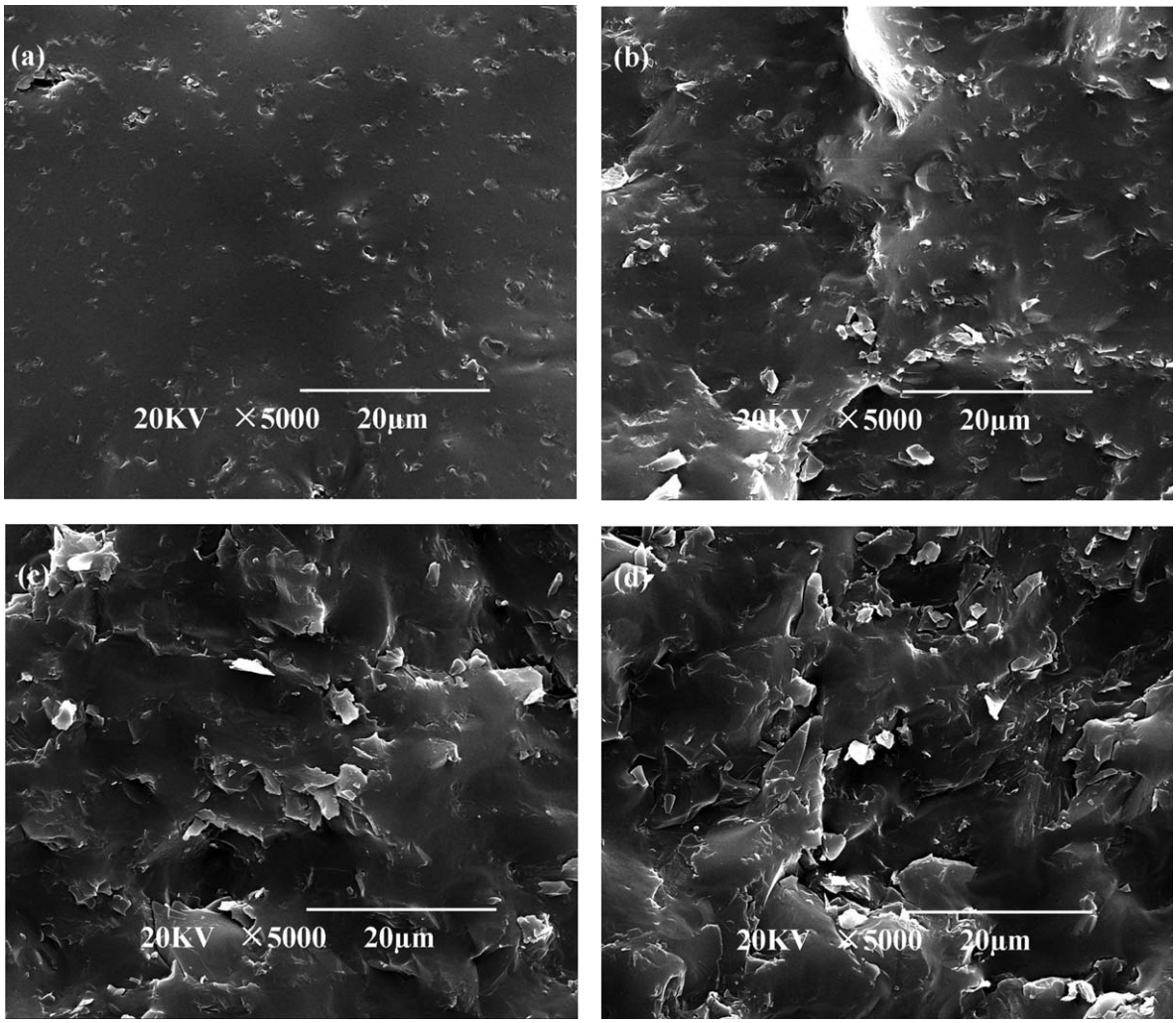

Figure 4. SEM image of CIIR with different C9 resin contents: (a) CIIR/25 phr C9 resin, (b) CIIR/50 phr C9 resin, (c) CIIR/75 phr C9 resin, (d) CIIR/100 phr C9 resin.

blends are much broader than that of pure CIIR; the glass transition of CIIR is barely detectable when the C5 resin content reaches 100 phr. This phenomena is caused by concentration fluctuation and depressing the free motion of CIIR.[14] For the CIIR/C9 resin blends, the glass transition of C9 resin still can be observed in the heat flow curves, and the glass transition of CIIR slightly moves to high temperature from Figure 2, indicating that the miscibility between CIIR and C9 resin is poor due to the existence of a larger number of phenyl rings on C9 resin molecular chain, so that the glass transition of CIIR moves to high temperature very slightly.

Morphology of CIIR/Petroleum Resin Blends

The phase morphology of the CIIR/aliphatic C5 resin blends with increase in the content of C5 resin is observed with SEM as presented in Figure 3. The micrographs of pure CIIR and CIIR with 25phr PR blend show a single-phase morphology [Figure 3(a,b)], whereas PR content is more than 50 phr, reaching saturation in the blends; a few rich C5 resin domains emerge, then dual-phase morphology with PR domains dispersed like "sea-islands" in the continuous CIIR matrix is observed [Figure 3(c–e)]. The average dimension of C5 resin domains increases from 5.6 μm to 8.7 μm with its content going up from 50 phr to 100 phr, and the amount of C5 resin sea-island domains also increases obviously. The C5 resin disperses in the CIIR chains when the resin content is lower, but this kind of dispersion is decreased when the CIIR is saturated with C5 resin. It suggests that the CIIR and C5 resin is miscible to a certain extent. And these morphological features are in accord with the evidences from DSC and DMA results; the Tg of CIIR firstly increases and then increases very slowly after the C5 resin content is more than 50 phr. Although phase separation of blends emerges with increase in the content of C5 resin, there is neither a striking split of peak in the tan δ curves of DMA data nor can the loss peak of C5 resin be detected. As shown in Figure 4, the morphological feature of the CIIR/aromatic C9 resin blends is observed that all the blends exhibit dual-phase morphology with C9 resin domains dispersed in the CIIR matrix. Nevertheless, because the miscibility between C9 resin and CIIR is poorer and the interaction between C9 resin

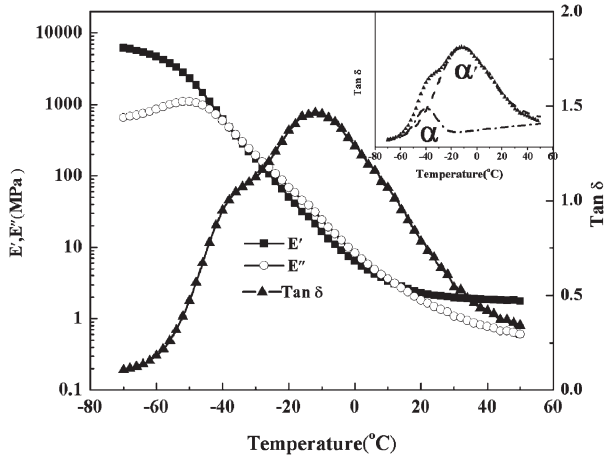

Figure 5. Dynamic mechanical spectra of CIIR at 10 Hz. The upper inset shows that the loss tangent peak of CIIR is resolved into two peaks using a nonlinear fitting method. The first peak refers to the shoulder, as shown by the dash-dot line. The latter peak refers to the main peak, as shown by the dash line.

and CIIR is weaker than that between C5 resin and CIIR, as a result, the C9 resin domains can be observed even when the content is only 25 phr [Figure 4(a)], and the average dimension of C9 resin domains increases significantly with its content going up from 25 phr to 100 phr [Figure 4(a–d)], which is much larger than that of aliphatic C5 resin at the same content. Simultaneously, the interface between CIIR and C5 resin is fuzzier than that of CIIR and C9 resin. This also explains why the glass transition of C9 resin is observed in the DSC curves and the glass transition of CIIR in the blends only slightly moves.

Dynamic Mechanical Property of CIIR

DMA measurement, which is sensitive to all the different modes of molecular motion, has been extensively used to detect the change of molecular dynamics of polymer composites with the variation of added composition contents. The dynamic mechanical spectra of CIIR at 10 Hz are shown in Figure 5. The loss modulus (E″) shows a peak at −50.5°C, but the tan δ maximum of CIIR is a lag behind the E″ peak about 38°C. For other polymers, the lagged value is only about 10–20°C; this phenomenon is interpreted in terms of the effective chain packing. It can be observed that tan δ peak of CIIR displays an asymmetrical broaden peak with a shoulder at about −33.5°C and a maximum at −12.4°C. However, taking the temperature of the maximum of the isochronal tan δ peak as Tg is problematic, because tan δ peak in the glass-to-rubber transition region involves not only local segmental dynamics, which determines the glass transition temperature, but also sub-Rouse modes and Rouse modes, as suggested by Ngai, Plazek, Donth et al.[8,18] On the basis of literatures,[19,20] the tan δ peak can be resolved into two peaks by a nonlinear fitting method, as shown in the upper inset of Figure 5; the resolved first peak at lower temperature causes the shoulder, while the latter peak at higher temperature gives rise to the maximum. The two loss peaks correspond to α and α' transition; the α process is the correlated motion of local segments, which determines the Tg of CIIR, while the slow α' process should be attributed to the motion of longer chain segments composed of the sub-Rouse modes and the Rouse modes, which usually involve the motion of chain segments containing about 10–50 or more backbone bonds. Obviously, the loss peak of the slow α' process is more effective to the CIIR damping

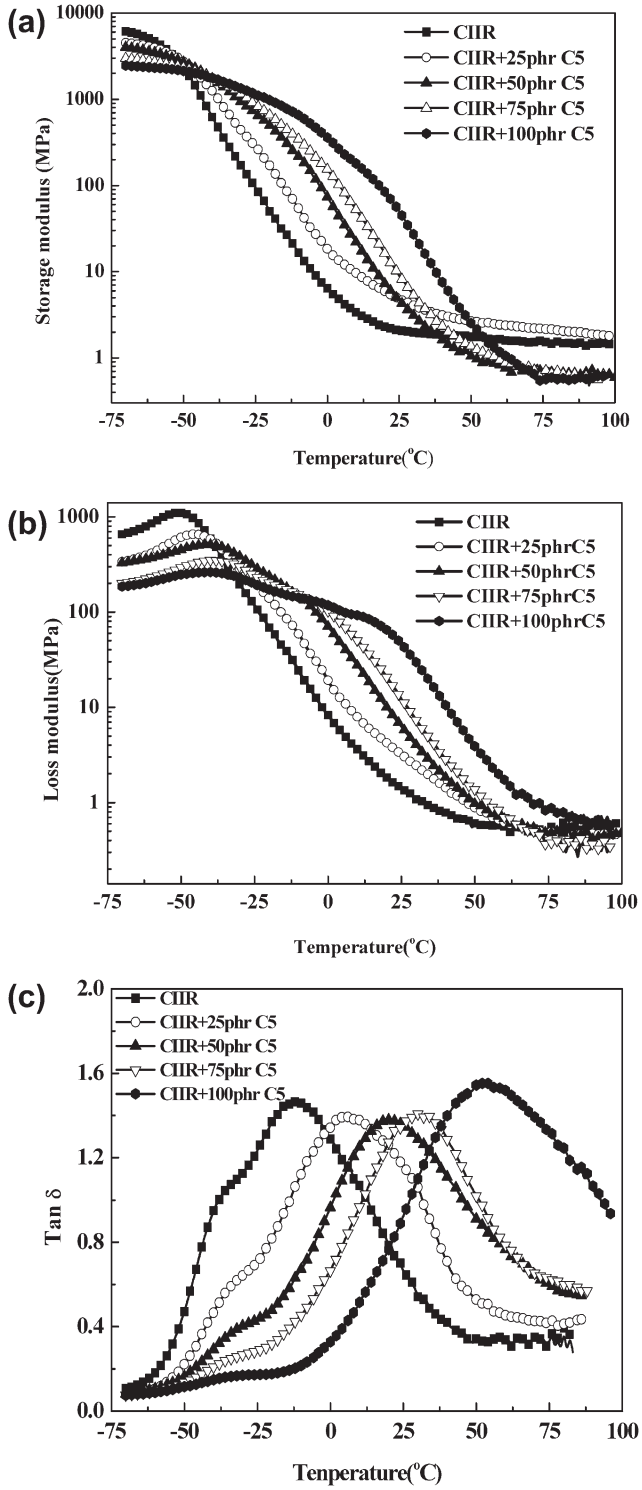

Figure 6. Storage modulus (a), loss modulus, (b) and tan δ, (c) versus temperature curves with different C5 resin contents.

Table 1. Effect of C5 Resin Content on the Loss Peak Position and Height of α and α′ Processes of CIIR

Samples	Tg-DSC (°C)	Tan δ peak position (°C)		Tan δ peak height	
		α process	α′ process	α process	α′ process
CIIR	−62.6	−33.5	−12.4	1.06	1.46
CIIR + 25 phr C5	−60.6	−32.0	0.6	0.63	1.39
CIIR + 50 phr C5	−58.0	−31.0	18.1	0.40	1.38
CIIR + 75 phr C5	−57.8	−29.9	32.9	0.27	1.41
CIIR + 100 phr C5	−57.0	−29.5	50.2	0.17	1.55

materials. However, both of the loss peaks appear at lower temperature zone than room temperature.

Effect of C5 Resins on Damping Property of CIIR

The storage modulus (E′), loss modulus (E″) and tan δ curves of CIIR with different aliphatic C5 resin contents are shown in Figure 6. In the wide range of −40 to 40°C, where the glass–rubber transition of CIIR locates, the storage modulus and loss modulus schematically rise up with increasing PR contents significantly, and the maximum of loss modulus shifts toward higher temperature. Simultaneously, it can be seen from that the E′ curve of CIIR/100 phr C5 blend shows a more obvious high-temperature inflexions and the E″ also shows a new peak at about 25°C, which is related to glass transition of C5 resin-rich domains in the blends. Due to the remarkable change of storage modulus and loss modulus, the shape of the tan δ peak is significantly altered with increase in the content of C5 resin in the blends; the asymmetrical peak of CIIR becomes wider and wider. Especially, the blends with 25 phr and 50 phr C5 resin exhibit high damping factor and wide efficient damping temperature range (tan $\delta > 0.5$) at room temperature. Both the α process and α′ process of CIIR move to the higher temperature but to different extents.

It can be noticed from Table 1 that the relaxation temperature of α process firstly increases, and then increases very slowly after the C5 resin content reaching 50 phr. At the same time, the relaxation temperature of α′ process shifts dramatically toward higher temperature with increase in the PR content. For the pure CIIR, the temperature difference of Tα and Tα′ is only about 21°C, hence it is not easy to separate independently the contribution of each mode from one another, because the relaxation process of the different molecular motion modes is overlapped. The temperature difference of Tα and Tα′ of CIIR blend with 50 phr C5 resin is about 48°C; therefore, in the dynamical mechanical spectrum of CIIR, different modes of molecular motion are more clearly discerned. On the contrary, the loss peak height of the α process is dramatically suppressed with the CIIR content decreasing in the blends, but the height of the maximum is little changed, which is related to the possibility that the molecular chains relaxation of α′ process requires more energy and converts more mechanical vibration energy to heat energy.

As is reported previously, the α process that contains 2 or 3 backbone bonds needs small free volume, while the α′ process that contains in the order of 50 or more backbone bonds needs more larger free volume than the α′ process. As a result, the α process and α′ process have different responses to the space limited by blending with other polymers or fillers. On the basis of the results, it is interesting to define that C5 resin molecular chains and rich domains form space confinement on the CIIR chains, and this space confinement should affect these peaks to different extents. And the presence of C5 resin molecules slightly confines the molecular mobility of the local segments of CIIR, but greatly confines the molecular mobility of the Rouse modes of CIIR; in this case, the relaxation of molecular chain requires more energy, which results shoulder and the maximum of the loss peak move toward high temperature with different extents in the dynamic mechanical spectra. And the slight phase separation of dispersed C5 resin with several micron diameters can still confine α′ process (or Rouse modes) with long scales, but has little influence on the local segmental motion, which needs rather small free volume. The different confinement effects on different scale molecular chain relaxations also happen in the CIIR and phenolic resin vulcanized damping materials in which the linear phenolic resin is partially miscible with CIIR.[21]

Effect of C9 Resins on Damping Property of CIIR

The effect of mixing ratio of CIIR/C9 resin on the relaxation behavior of CIIR at 10 Hz is exhibited in Figure 7. There are two inflexions observed from the E′ curves of the blend, and two peaks observed from E″ curves. The transition located at low temperature corresponds to the CIIR matrix obviously, and the transition located at high temperature corresponds to the C9 resin-dispersed phase. Both E′ and E″ at the range from CIIR glass transition to C9 resin glass transition gradually increase as the content of C9 resin increases in the blend, and the maximum of loss modulus almost remains unchanged.

It is clear from Figure 7(c) that the CIIR/C9 blends show two tan δ peaks, which is the indication of immiscibility. With increase in the content of C9 resin in the blends, the shoulder, and the maximum values of tan δ peak, which correspond to CIIR α process and α′ process, move slightly to high temperature. Both of them are suppressed but to different extents, the tan δ peak corresponding to C9 resin, which is located at about 108°C, rises up at the same time.

This is quite different from the dynamic mechanical behaviors of CIIR/C5 resin blends. The effect of C9 resin content on the peak height and position of the α process and α′ process of CIIR are displayed in Table 2. It can be observed that the

temperature position of the α process and that of the α′ process move to high temperature very slightly by adding the C9 resin. This is due to the fact that the interaction between CIIR and C9 resin is weak and the C9 resin phase domains with larger dimension cannot confine the motion of CIIR molecular chains. The height of the α′ process is dramatically reduced; on the contrary, that of the α process is slowly depressed. The reason is

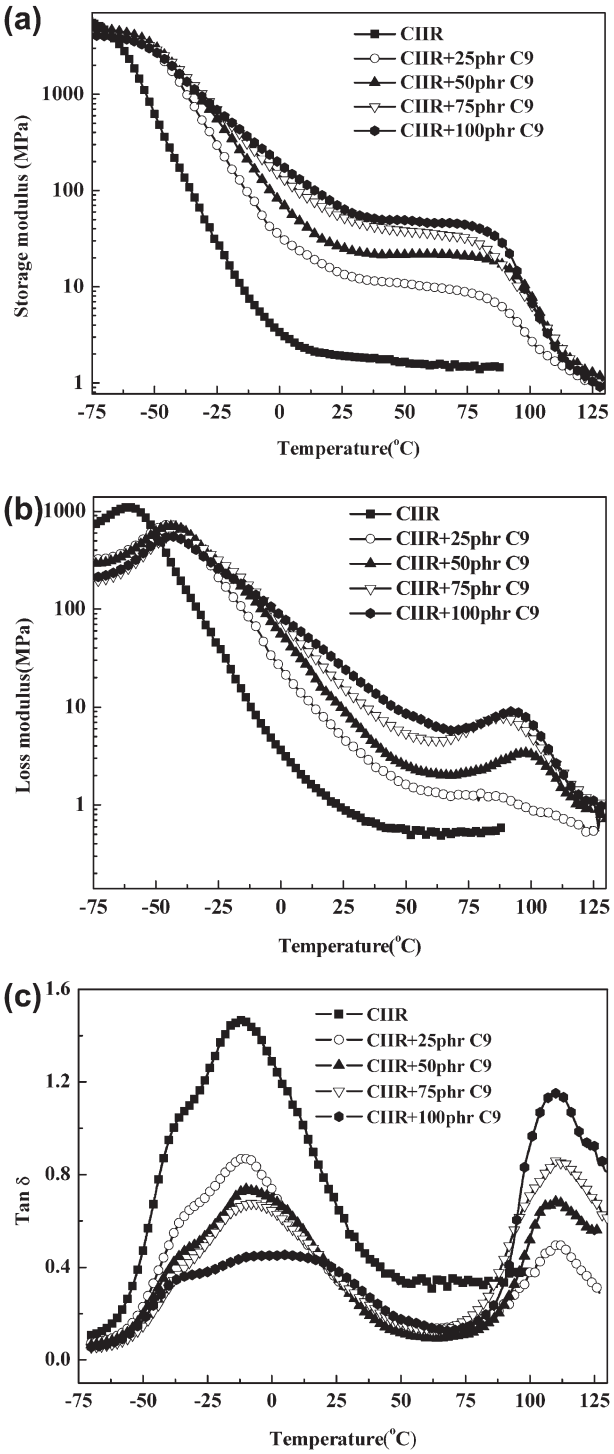

Figure 7. Storage modulus (a), loss modulus, (b) and tan δ, (c) versus temperature curves with different C9 resin contents.

Table 2. Effect of C9 Resin Content on the Loss Peak Position and Height of α and α′ Processes of CIIR

		Tan δ peak position (°C)		Tan δ peak height	
Samples	Tg-DSC (°C)	α process	α′ process	α process	α′ process
CIIR	−62.6	−33.5	−12.4	1.06	1.46
CIIR + 25 phr C9	−61.2	−32.8	−11.4	0.66	0.87
CIIR + 50 phr C9	−60.9	−31.6	−10.5	0.5	0.74
CIIR + 75 phr C9	−60.6	−32.0	−10.9	0.41	0.66
CIIR + 100 phr C9	−59.6	−32.1	−10.5	0.36	0.45

that the glass transition temperature of C9 resin (62°C) is much higher than the glass transition temperature (−62.6°C), and the C9 resin domains dispersed in CIIR matrix have different effect on different molecular motion modes with different length scales. Here, the limited free volume again plays an important role. It has been reported that the thermal stress is relatively high on the interface in immiscible polymer blends; as a result, the free volume expansion of CIIR is limited, which suppresses the motion of longer chain segments more significantly.[13]

Because C9 resin neither moves loss peak of CIIR to room temperature nor enhances values of tan δ peak, it is not suited to incorporating with CIIR for improving damping property. Furthermore, a large number of benzene may lead C9 resin more suitable to polymers containing benzene, such as SIS/C9 resin-damping materials reported in the literatures.[17] Hence, the moderate miscibility is a positive impact on the damping property of CIIR/petroleum resin blends, and not all of the petroleum resins, which have various and complex structure types, are suited to incorporating with CIIR for improving damping property. And the moderate miscibility is a positive impact on the damping property of CIIR/petroleum resin blends.

CONCLUSION

The aliphatic C5 resin exhibits a better miscibility with CIIR, compared with aromatic C9 resin. Small amounts of C5 resin are miscible with CIIR; the rich C5 resin domains emerge when CIIR is saturated with resin. With increment in C5 resin content, the α process and the α′ process of loss peak of CIIR move to the higher temperature but to different extents, because the presence of C5 resin molecules slightly confines the molecular mobility of the α process of CIIR, but greatly confines the molecular mobility of the slow α′ process of CIIR that contains more backbone bonds.

The miscibility between CIIR and C9 resin is poor owning to the existence of larger number of phenyl rings on C9 resin molecular chain. The loss peak of CIIR moves to high temperature very slightly with the addition of C9 resin. The loss peak

height of the α' process relaxation is more dramatically reduced, than that of the α process, because the free volume expansion of CIIR is limited, which suppresses the motion of longer chain segments more significantly.

ACKNOWLEDGMENTS

Financial supports of the National Natural Science Foundation of China (51273132, 51227802 and 51121001) and Program for New Century Excellent Talents in University (NCET-13-0392) are gratefully acknowledged.

REFERENCES

1. Ratna, D.; Manoj, N.; Chandrasekhar, L.; Chakraborty, B. *Polym. Adv. Technol.* **2004**, *15*, 583.
2. Clarke, S. M.; Tajbakhsh, A. R.; Terentjev, E. M.; Remillat, C.; Tomlinson, G. R.; House, J. R. *J. Appl. Phys.* **2001**, *89*, 6530.
3. Liang, J. Y.; Chang, S. Q.; Feng, N. *J. Appl. Polym. Sci.* **2013**, *130*, 510.
4. Mao, X. D.; Xu, S. A.; Wu, C. F. *Polym. Plast. Technol.* **2008**,*47*, 209.
5. Li, C.; Xu, S. A.; Xiao, F. Y.; Wu, C. F. *Eur. Polym. J.* **2006**, *42*, 2507.
6. Li, C.; Wu, G. Z.; Xiao, F. Y.; Wu, C. F. *J. Appl. Polym. Sci.* **2007**, *106*, 2472.
7. Fitzgerald, E. R.; Grandine, L. D.; Ferry, J. D. *J. Appl. Phys.* **1953**, *24*, 650.
8. Plazek, D. J.; Chay, I. C.; Ngai, K. L.; Roland, C. M. *Macromolecules.* **1995**, *28*, 6432.
9. Wu, J. R.; Huang, G. S.; Wang, X. A.; He, X. J.; Zheng, J. *Soft Matter.* **2011**, *7*, 9224.
10. Wang, X. A.; Huang, G. S.; Wu, J. R.; Nie, Y. J.; He, X. J. *J. Phys. Chem. B.* **2011**, *115*, 1775.
11. Liao, F. S.; Su, A. C.; Hsu, T. C. *Polymer.* **1994**, *35*, 2579.
12. Huang, G. S.; He, X. R.; Wu, J. R.; Pan, Q. Y.; Zheng, J.; Hong, Z.; Jiang, L. X.; Zhao, X. D. *J. Appl. Polym. Sci.* **2006**, *102*, 3127.
13. Wu, J. R.; Huang, G. S.; Wang, X. A.; He, X. J.; Lei, H. X. *J. Polym. Sci. Part B: Polym. Phys.* **2010**, *48*, 2165.
14. Wu, J. R.; Huang, G. S.; Wang, X. A.; He, X. J.; Lei, H. X. *J. Polym. Res.* **2011**, *18*, 2213.
15. Kim, J. K., Ryu, D. Y.; Lee, K. H. *Polymer.* **2000**, *41*, 5195.
16. Liang, J. Y.; Chang, S. Q.; Feng, N. *J. Appl. Polym. Sci.* **2013**, *130*, 510.
17. Wu, C. Y.; Wu, G. Z.; Wu, C. F. *J. Appl. Polym. Sci.* **2006**, *102*, 4157.
18. Plazek, D. J.; Ngai, K. L. Physical Properties of Polymers Handbook; James, E. M., Ed.; Springer: New York, **2007**; Vol. 1, Chapter 12, pp 187–215.
19. Wu, J. R.; Huang, G. S.;Qu, L. L.; Zheng, J. *J. Non-Cryst. Solids.* **2009**, *355*, 1755.
20. Wu, X.; Zhu, Z.; *J. Phys. Chem. B.* **2009**, *113*, 11147.
21. Qu, L. L.; Huang, G. S.; Wu, J. R.; Tang, Z. H. *J. Mater. Sci.* **2007**, *42*, 7256.